

polymer papers

Small-angle X-ray scattering from high-density polyethylene: lamellar thickness distributions

Carla Marega, Antonio Marigo, Gianmatteo Cingano and Roberto Zannetti*

Dipartimento di Chimica Inorganica, Metallorganica ed Analitica dell'Università di Padova, via Loredan 4, 35131 Padova, Italy

and Guglielmo Paganetto

*Centro Ricerche 'Giulio Natta' della Montell-Italia, 44100 Ferrara, Italy
(Received 6 February 1995; revised 10 October 1995)*

Small-angle X-ray diffraction patterns were recorded for a number of high-density polyethylene samples and were successively analysed by a fit with the calculated patterns corresponding to certain theoretical models. The parameters determined by the above fits were as follows: long-period, crystallinity, mean dimensions of the crystalline lamellae, amorphous thickness, crystallinity and lamellar dimension distributions. Regarding the latter, two mathematical functions were used for the fits, i.e. a symmetrical and an asymmetrical type, and for all of the samples examined the function was determined which gives the best results. Finally, a correlation is suggested between the polymer molecular weight and lamellar dimension distributions. Copyright © 1996 Elsevier Science Ltd.

(Keywords: small-angle X-ray scattering; lamellar thickness distribution; high-density polyethylene)

INTRODUCTION

Small-angle X-ray scattering (SAXS) from crystalline polymers can give rise to rather broad peaks, which are interpretable in terms of one-dimensional models, based upon regular arrays of alternating crystalline (lamellae) and amorphous regions.

The structural analysis of such peaks by the application of Bragg's law allows an evaluation of the corresponding long-period, but this is a rather simplified approach which, for broad peaks, provides a long-period value which is affected by a number of errors when compared to the true lamellar periodicity.

Some theoretical models, described in the literature¹, allow a more satisfactory analysis of the above broad peaks based upon a distribution of the lamellar thickness and on the assumption that such a distribution can be described by symmetrical or asymmetrical functions. These models assume infinite lateral dimensions of the lamellae, and hence they account only for the electron density change along the stacking direction (normal to the lamellae) of the crystalline and amorphous boundary layers. Furthermore, the models take into account a finite or an infinite number of layers, which are characterized by a sharp electron-density transition at the crystal–amorphous interface.

Some of these theoretical models were tested in

investigations of low-density polyethylene^{1,2}, and in the present work they are applied to the analysis of high-density polyethylene (HDPE): actually, in this present work they were introduced into a minimization routine, in order to reach not only an evaluation of the best model, but also the calculation of the corresponding parameters giving the best fit of the SAXS peaks, i.e. the mean thickness of the crystalline and amorphous layers, their statistical distribution, the percentage crystallinity of the sample and finally, for some models, the crystallinity distribution.

THEORETICAL CONSIDERATIONS

In the considered theoretical models, a lamellar stacking is assumed to have an infinite lateral width: as a consequence, a one-dimensional variation is considered for the electron density. Furthermore, the models assume a simplified two-phase structure, where crystalline and amorphous regions are obviously introduced, but transition layers are not considered: this schematic model is represented in *Figure 1*, where the crystalline thickness, the amorphous thickness and the total periodicity of the *i*th lamella are indicated by Y_i , Z_i , and X_i , respectively.

The statistical fluctuation of the electron density along the lamellar normal can be described by the Hosemann's model³, where an independent variation is introduced for both of the crystal and amorphous region thicknesses.

* To whom correspondence should be addressed

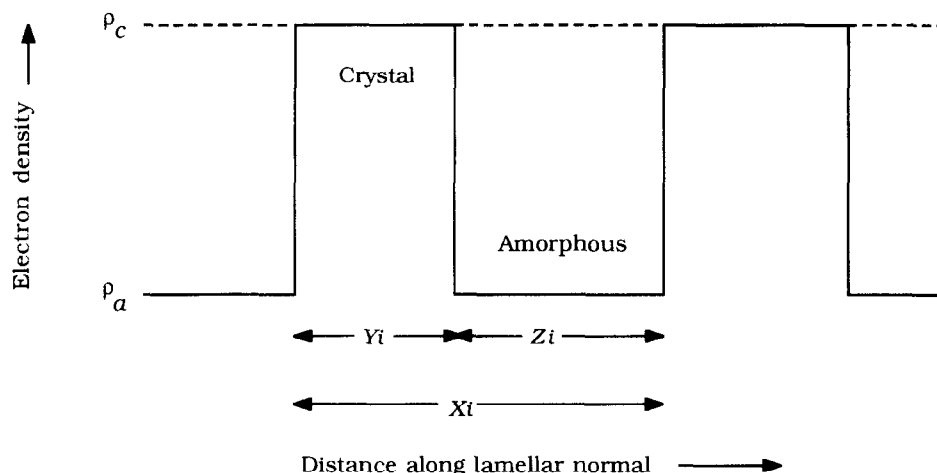


Figure 1 Basic model for a lamellar stack

According to this model, the intensity profile is given by the following:

$$I(s) = I_B(s) + I_C(s) \quad (1)$$

where:

$$I_B(s) = \frac{(\rho_c - \rho_a)^2}{4\pi^2 s^2 \bar{X}} \times \frac{|1 - F_Y|^2(1 - |F_Z|^2) + |1 - F_Z|^2(1 - |F_Y|^2)}{|1 - F_Y F_Z|^2} \quad (2)$$

$$I_C(s) = \frac{(\rho_c - \rho_a)^2}{2\pi^2 s^2 \bar{X} N} \times \text{Re} \left\{ \frac{F_Z(1 - F_Y)^2(1 - (F_Y F_Z)^N)}{(1 - F_Y F_Z)^2} \right\} \quad (3)$$

F_Y and F_Z are, respectively, the Fourier transforms of the distribution of the crystalline and amorphous thicknesses, $s = (2 \sin \theta) / \lambda$, ρ_c and ρ_a represent the electron densities of the crystalline and amorphous regions, respectively, and N is the number of lamellae along the stacks.

In this present paper, four different theoretical models were considered, and these are discussed below.

Simple lamellar stack model

The first model considered⁴ is based upon a single lamellar stacking which represents, according to a statistical formulation, the whole of the sample; furthermore, it assumes that the number of lamellae is so large that it can be considered as being infinite and as a consequence the term $I_C(s)$ of equation (1) can be neglected. With respect to the distribution of the thicknesses of the amorphous and crystalline layers, a symmetric, as well as an asymmetric function, were considered.

A typical symmetric distribution is provided by a Gaussian function such as the following:

$$H(Y) = \frac{1}{\sigma_Y(2\pi)^{1/2}} \exp \left[-\frac{(Y - \bar{Y})^2}{2\sigma_Y^2} \right] \quad (4)$$

where \bar{Y} and σ_Y are the average and the standard deviation of the crystal thicknesses. (A Gaussian function

will give a positive probability for negative values of Y in the negative tail: to avoid this, it is sufficient to consider $\sigma_Y < 0.5\bar{Y}$.)

The corresponding Fourier transforms are as follows:

$$F_Y = \exp(-2\pi^2 s^2 \sigma_Y^2) \exp(-2\pi i s \bar{Y}) \quad (5)$$

with the analogous functions, $H(Z)$ and $F(Z)$, referring to the amorphous thickness.

The overall average long-period is $\bar{X} = \bar{Y} + \bar{Z}$, and the volume crystallinity of the system is $\Phi = \bar{Y}/\bar{X}$; finally, σ_Y and σ_Z are related by the following formula¹:

$$\sigma_Y / \bar{Y} = \sigma_Z / \bar{Z} \quad (6)$$

Among the asymmetrical functions, the exponential one was considered: in particular, in this present work, a modified exponential distribution¹ was used, as follows:

$$H(Y) = \frac{1}{\sigma_Y} \exp \left[-\frac{(Y - Y_0)}{\sigma_Y} \right] \quad \text{for } Y \geq Y_0 \\ = 0 \quad \text{for } Y < Y_0 \quad (7)$$

where the average thickness $\bar{Y} = Y_0 + \sigma_Y$.

The Fourier transforms of this distribution can be represented in the following form:

$$F_Y = \frac{1}{1 + 2\pi i s \sigma_Y} \exp(-2\pi i s Y_0) \quad (8)$$

Figures 2 and 3 show the calculated SAXS intensity curves corresponding to different standard deviations and for both a Gaussian and an exponential distribution, respectively.

The theoretical intensity profiles were evaluated by putting $X = 1.0$ on a length scale L , and the average crystal thickness was set to be $0.5L$; furthermore, for simplicity, $\sigma_Y = \sigma_Z = \sigma$.

In the second model, a discrete number (N) of lamellae is introduced, which broadens the peaks, owing to the finite lattice size¹; under this hypothesis, it is no longer possible to neglect the $I_C(s)$ term of equation (1).

Variable stack model

A third model was considered, where an infinite number (N) of lamellae is introduced; however, it is assumed that there is a longer-range inhomogeneity than in the single stack model, in which there are fluctuations

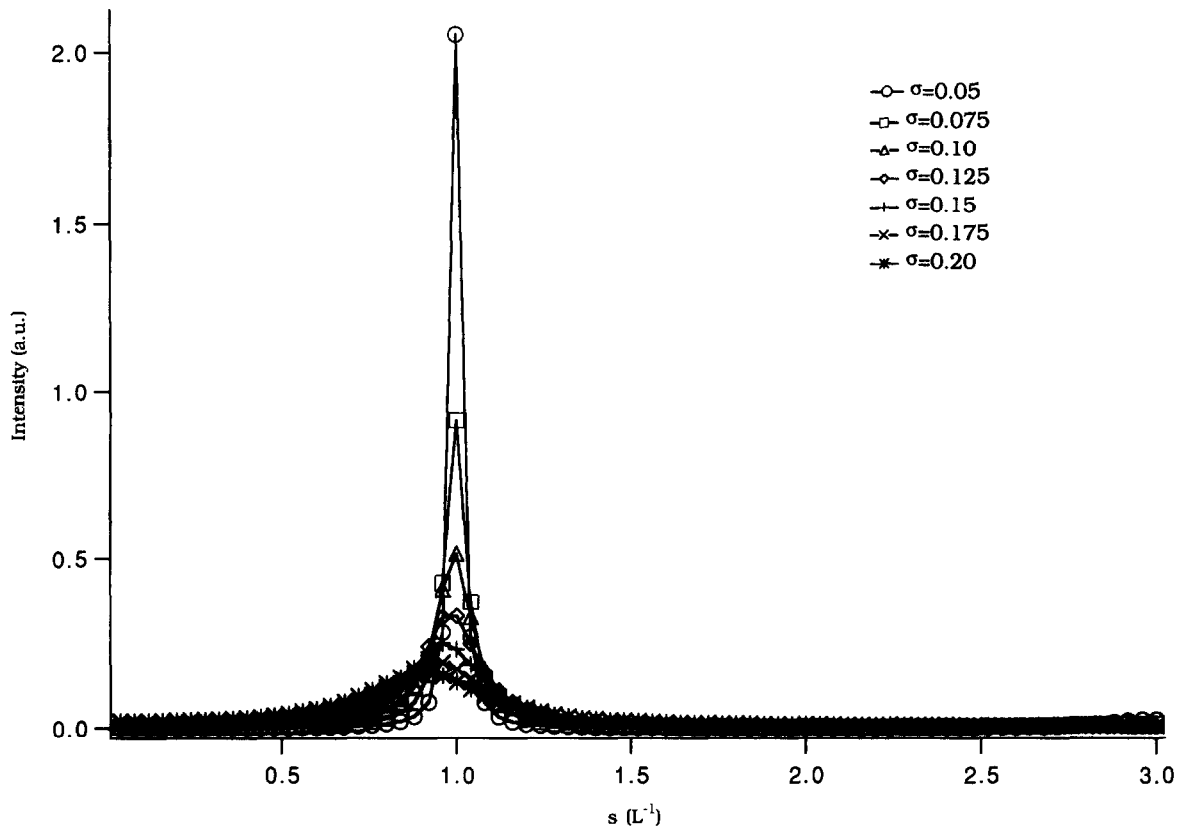


Figure 2 Calculated SAXS intensity curves based on the simple stack model with Gaussian thickness distributions

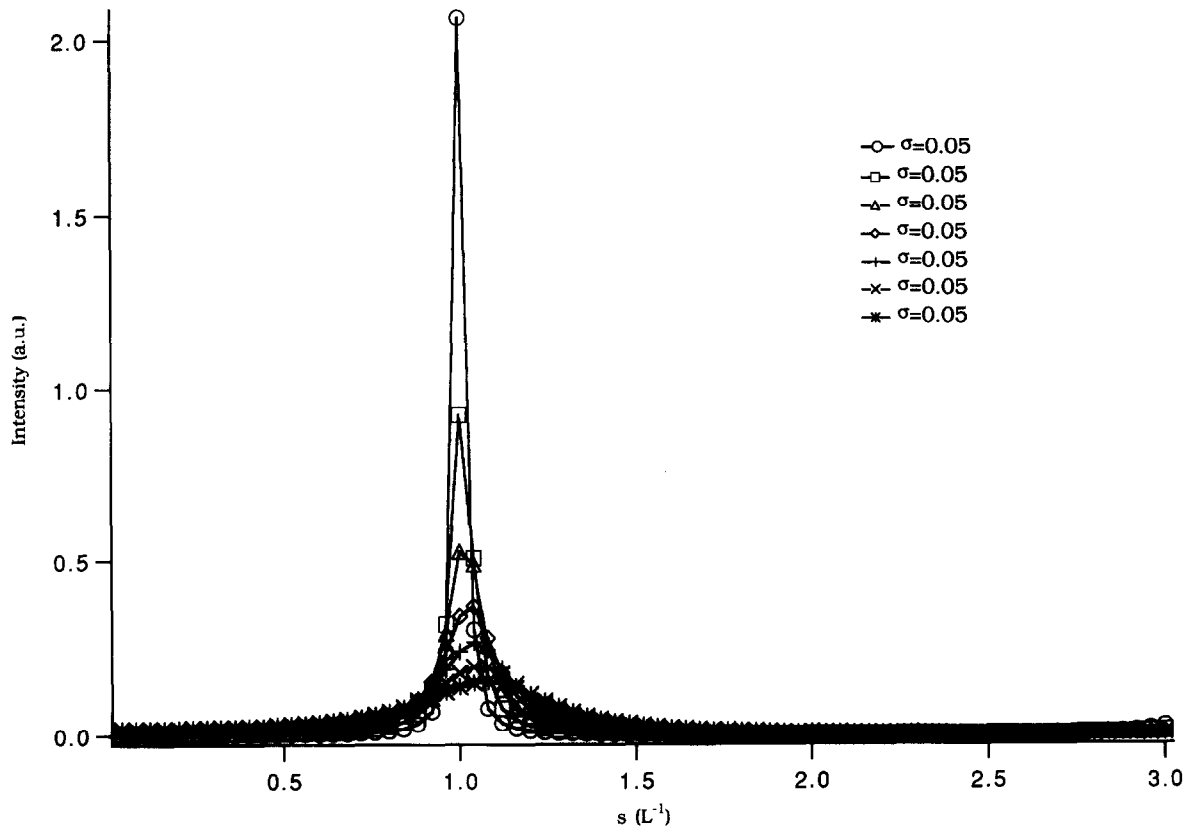


Figure 3 Calculated SAXS intensity curves based on the simple stack model with exponential thickness distributions

among the stacks, as well as fluctuations within each stack.

The SAXS scattering is evaluated as the weight-average on all of the stacks: the model was proposed by Strobl and Muller⁵, and was used in a particular form by Blundell¹, who considered a change in the local crystallinity between stack and stack.

The crystallinity fluctuation in the sample is given by a normalized distribution function $P(\Phi)$, which represents the probability that a well defined crystallinity is associated with a well determined stack volume. The intensity is then represented as follows:

$$I(s) = \int I(s, \Phi) P(\Phi) d\Phi \quad (9)$$

where it is assumed that $P(\Phi)$ follows a Gaussian distribution. Moreover, it is assumed that the average thickness of the amorphous regions remains constant, while, in contrast, the average crystal thickness of each stack follows the distribution determined by $P(\Phi)$.

Finally, the last (fourth) model considered introduces into the calculations a finite number (N) of lamellae.

EXPERIMENTAL

Samples

Homopolymer samples of high-density polyethylene (HDPE) were synthesized by a suspension process, using a Ziegler–Natta catalyst (TiCl_4 supported on MgCl_2 and activated by AlEt_3 in *n*-hexane as solvent). Samples for the wide-angle X-ray scattering (WAXS) and SAXS measurements were prepared by melting in a heated die for 10 min at 150°C, after which the melted polymers were crystallized at 100°C for 60 min (PEa, PEb, PEc, PEd) and at 130°C for 90 min (PEc(iso), Ped(iso)) (see Table 1), and finally cooled to room temperature. After this treatment, plates were obtained having a 2.5 mm thickness. The density d (g cm^{-3}) of the plates was determined by a suitable density gradient column.

The number-average (M_n) and weight-average (M_w) molecular weights (see Table 1) were evaluated by gel permeation chromatography in a Spherosil column (10^3 – 10^7 Å, 37–75 μm), using 1,2-dichlorobenzene as the eluent.

Wide-angle X-ray scattering

WAXS patterns were recorded in the diffraction angular range, $2\theta = 5$ – 120° , by a Seifert MZ III powder diffractometer equipped with a graphite curved-crystal monochromator on the diffracted beam; $\text{CuK}\alpha$ radiation was employed. Application of the Vonk

procedure⁶ gave values for the crystallinity by weight, Φ_{WAXS} , of the samples, while the volume crystallinity, Φ_{VOL} , was evaluated by using the following equation⁷:

$$\Phi_{\text{VOL}} = 1 / \left(1 + \frac{1 - \Phi}{\Phi} \frac{d_c}{d_a} \right) \quad (10)$$

where the crystal density d_c was determined by WAXS, as described below, while for the amorphous density a value for d_a of 0.85 g cm^{-3} was assumed⁷.

Small-angle X-ray scattering

SAXS patterns were recorded by a Kratky camera, using $\text{CuK}\alpha$ radiation produced by a Philips PW 1830 X-ray generator. The SAXS spectra were recorded by a Braun position-sensitive detector, over the scattering angular range $2\theta = 0.1$ – 5.0° , and were successively corrected for blank scattering.

A constant continuous background scattering⁸ was subtracted and the obtained intensity values, J , were smoothed, in the tail region, with the aid of the $sJ(s)$ versus $1/s^2$ plot. The Vonk desmearing procedure⁹ was then applied and the one-dimensional scattering function was obtained by the Lorentz correction: $J_1(s) = 4\pi s^2 J(s)$, where $J(s)$ is the desmeared intensity function and $s = (2 \sin \theta) / \lambda$.

The sum of the average thicknesses of the crystalline and amorphous regions was considered as the Bragg long-period, D_B , of the function $J_1(s)$; the average lamellar thickness was calculated, for an ideal two-phase model, by using the following equation¹⁰: $C_B = D_B \Phi_{\text{VOL}}$ (see Table 1).

Calculation procedure

The evaluation of the SAXS intensity corresponding to the considered models was carried out by the use of equation (1). The simulation algorithm is linked to the least-squares procedure MINUIT¹¹, in order to allow an evaluation of the main structural parameters. The goodness of each fit is given by R_{WP} , which accounts¹² for the weighted differences between the observed and calculated profiles. The parameters were optimized by a fit between the experimental and calculated SAXS patterns.

For the simple lamellar stack model, the optimized parameters were as follows:

- (1) the number, N , of lamellae;
- (2) the average thickness, \bar{Y} , of the lamellae;
- (3) the crystallinity, Φ ;
- (4) the standard deviation σ_Y , with reference to \bar{Y} .

Table 1 Values obtained for the molecular weights, crystallinity, identity period and average lamellar thickness of the HDPE samples examined in this study

Sample	M_n	M_w	M_w/M_n	Φ_{WAXS}	Φ_{Vol}	D_{Bragg} (Å)	C_B (Å)
PEa	17 200	149 000	8.6	0.759	0.726	326	236
PEb	16 200	121 000	7.5	0.766	0.734	310	227
PEc	16 200	83 000	5.1	0.794	0.764	283	216
PEc(iso)	16 200	83 000	5.1	0.814	0.788	368	290
PEd	23 600	374 000	15.8	0.739	0.705	326	230
PEd(iso)	23 600	374 000	15.8	0.787	0.758	349	265

The \bar{Z} and σ_Z values were evaluated by using the following:

$$\bar{X} = \bar{Y} + \bar{Z} \quad \text{and} \quad \Phi = \bar{Y}/\bar{X} \quad (11)$$

from which:

$$\bar{Z} = \left(\frac{1 - \Phi}{\Phi} \right) \bar{Y} \quad (12)$$

$$\sigma_Y/\bar{Y} = \sigma_Z/\bar{Z} \quad (13)$$

from which:

$$\sigma_Z = (\sigma_Y/\bar{Y})\bar{Z} \quad (14)$$

In the case of the variable stack model, the optimized parameters were as follows:

- (1) the number, N , of lamellae;
- (2) the crystallinity, Φ ;
- (3) the standard deviation σ_Φ , with reference to Φ ;
- (4) the average thickness, \bar{Z} , of the amorphous layer;
- (5) the standard deviation σ_Y , with reference to \bar{Y} .

The σ_Z value was determined as reported above, with \bar{Y} being given by the average of the calculated parameters according to the distribution $P(\Phi)$.

RESULTS AND DISCUSSION

The examined models were applied to the HDPE samples, by considering the distribution of the thicknesses of the crystalline and amorphous layers corresponding to both the Gaussian and exponential functions.

Table 2 R_{WP} parameters for the simple lamellar stack and variable stack models

Sample	R_{WP}		r^a (%)
	Simple stack model	Variable stack model	
PEa	0.0393	0.0161	59
PEb	0.0262	0.0223	15
PEc	0.0520	0.0249	52
PEc(iso)	0.0291	0.0107	63
PEd	0.0219	0.0113	48
PEd(iso)	0.0326	0.0170	48

^a Percentage reduction in R_{WP} for the variable stack model

The fits obtained for the simple lamellar stack model, both for $N = \infty$ and N being finite, generally show poor agreement. In *Table 2*, the best values are reported for R_{WP} corresponding to both the simple lamellar stack and the variable stack models.

Better results were obtained by using the variable stack model, both for the PE(a-d) and PE(c(iso),d(iso)) samples. The percentage reduction in R_{WP} for the latter model is also reported in *Table 2*. *Figure 4* shows the fits obtained for the various samples, while *Table 3* lists the values of the fit parameters.

First, it can be observed that for the PE(a-d) samples the data for the crystallinity Φ are comparable to the Φ_{VOL} values determined by WAXS, and that the standard deviations show low values, which are comparable for all of the samples; this could be expected if we consider that these PE homopolymer samples were prepared by following the same procedure.

Concerning the long-period parameter, good agreement can be observed for samples PEa and PEd, with lower values being obtained for the other two samples, particularly if one compares the above values with those obtained by applying Bragg's law. Moreover, it can be noted that the mean dimensions of the amorphous layers show a difference of only a few Å from sample to sample, but in contrast the dimensions of the crystalline lamellae show larger fluctuations.

However, different considerations need to be made concerning the samples obtained by isothermal crystallization. The crystallinity values obtained by the fits for PE(c(iso),d(iso)) show very good agreement with the data obtained from WAXS, and this is probably due to the fact that, owing to their thermal history, there are no amorphous or crystalline zones outside of the lamellar stacks in these samples.

The long-period and lamellar thickness values for PE(c(iso),d(iso)) are greater when compared to the corresponding values for PE(c,d), while the amorphous thickness values are comparable for PEd and PEd(iso); moreover, for PEc(iso) the thickness is less than that calculated for PEc.

Further comments can be made concerning the dimensions of the crystalline and amorphous layers: here it can be noted that for samples PEa, PEd and PEd(iso) the distribution which gives the best fit is the exponential one while for samples PEb, PEc and PEc(iso) the Gaussian one gives the best results. It can therefore be concluded that the lamellar distribution

Table 3 Best-fit parameters obtained for the HDPE samples examined in this study

Sample function	PEa exponential	PEb Gaussian	PEc Gaussian	PEc(iso) Gaussian	PEd exponential	PEd(iso) exponential
N	14	21	39	∞	43	59
Y	245	200	181	255	246	286
Z	83	83	88	69	90	96
X	328	283	269	324	336	382
Φ	0.746	0.707	0.674	0.787	0.733	0.749
σ_Y	35	64	47	93	44	69
σ_Z	12	27	23	25	16	23
σ	37	69	52	96	47	72
σ_Φ	0.06	0.05	0.05	0.03	0.07	0.09
R_{WP}	0.0161	0.0223	0.0249	0.0107	0.0113	0.0170

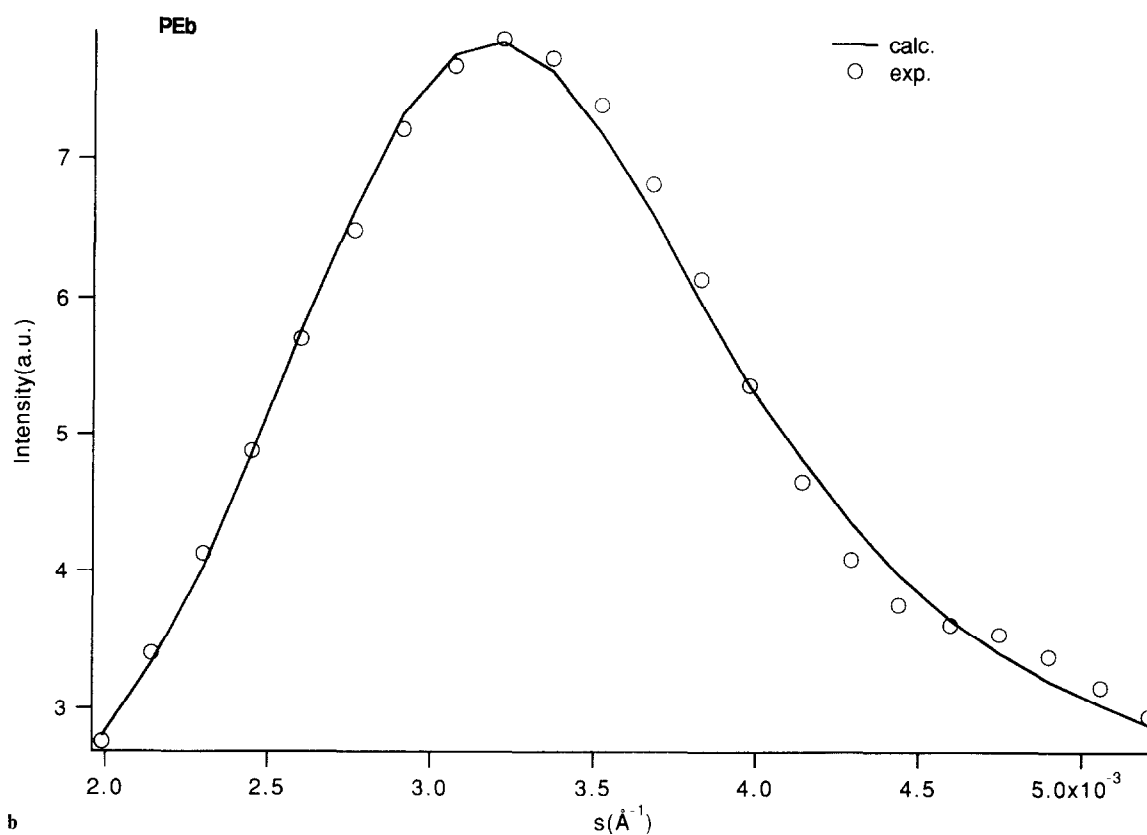
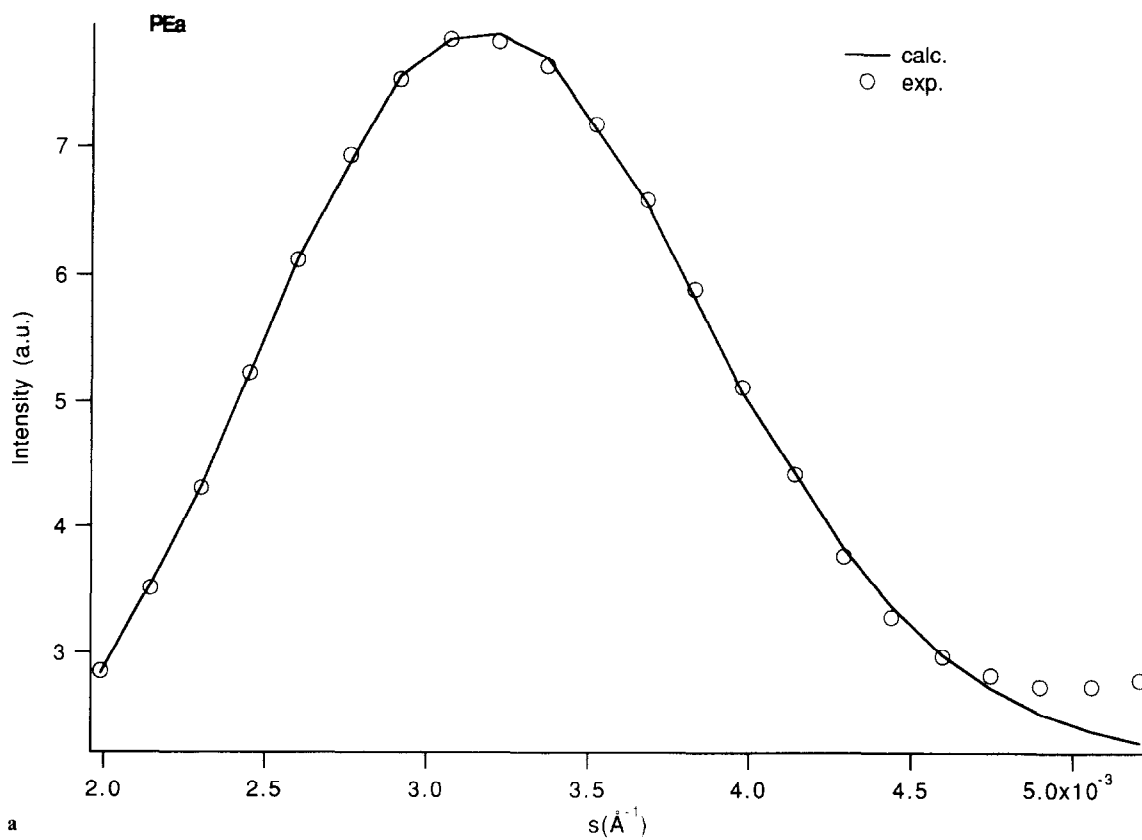


Figure 4 Best fits obtained between the observed and calculated SAXS intensity curves of the various samples: (a) PEa; (b) PEb; (c) PEC; (d) PEc(iso); (e) PED; (f) PED(iso). (Parameters are listed in Table 2)

function can show symmetrical or asymmetrical features, and that the kind of function describing this distribution must be evaluated in terms of each sample being examined.

Finally, if one considers the \bar{M}_w/\bar{M}_n ratios, reported in

Table 1, which provide an indication of the molecular-weight dispersion, it can be observed that within the same distribution type and the same sample preparation, i.e. by comparing the samples PEa and PEd, and PEb and PEc, a correlation is found between the behaviour of

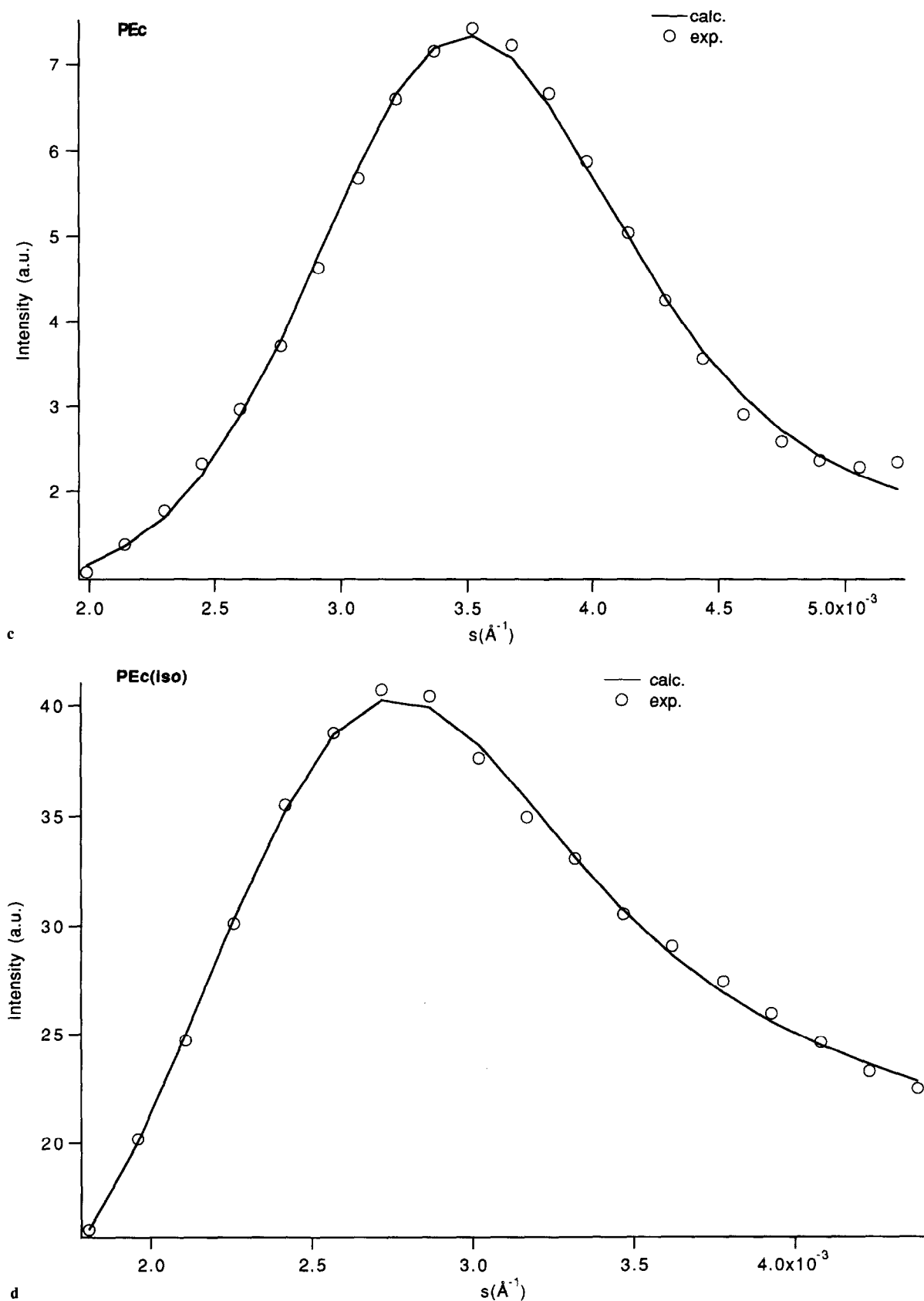


Figure 4 (Continued)

\bar{M}_w/\bar{M}_n and σ_Y and σ_Z : in effect, for a higher \bar{M}_w/\bar{M}_n ratio there are corresponding higher values of σ_Y and σ_Z .

Some analogous considerations can be made by examining the results obtained for all of the samples with respect to the same exponential function, even if for

PEc, and especially for PEb and PEc(iso), worse R_{WP} values can be noted when compared to the fit data relating to the Gaussian function (see Table 4).

Regarding the number of lamellae (N), values less than 50 were found for PE(a-d), while N is greater than 50 for

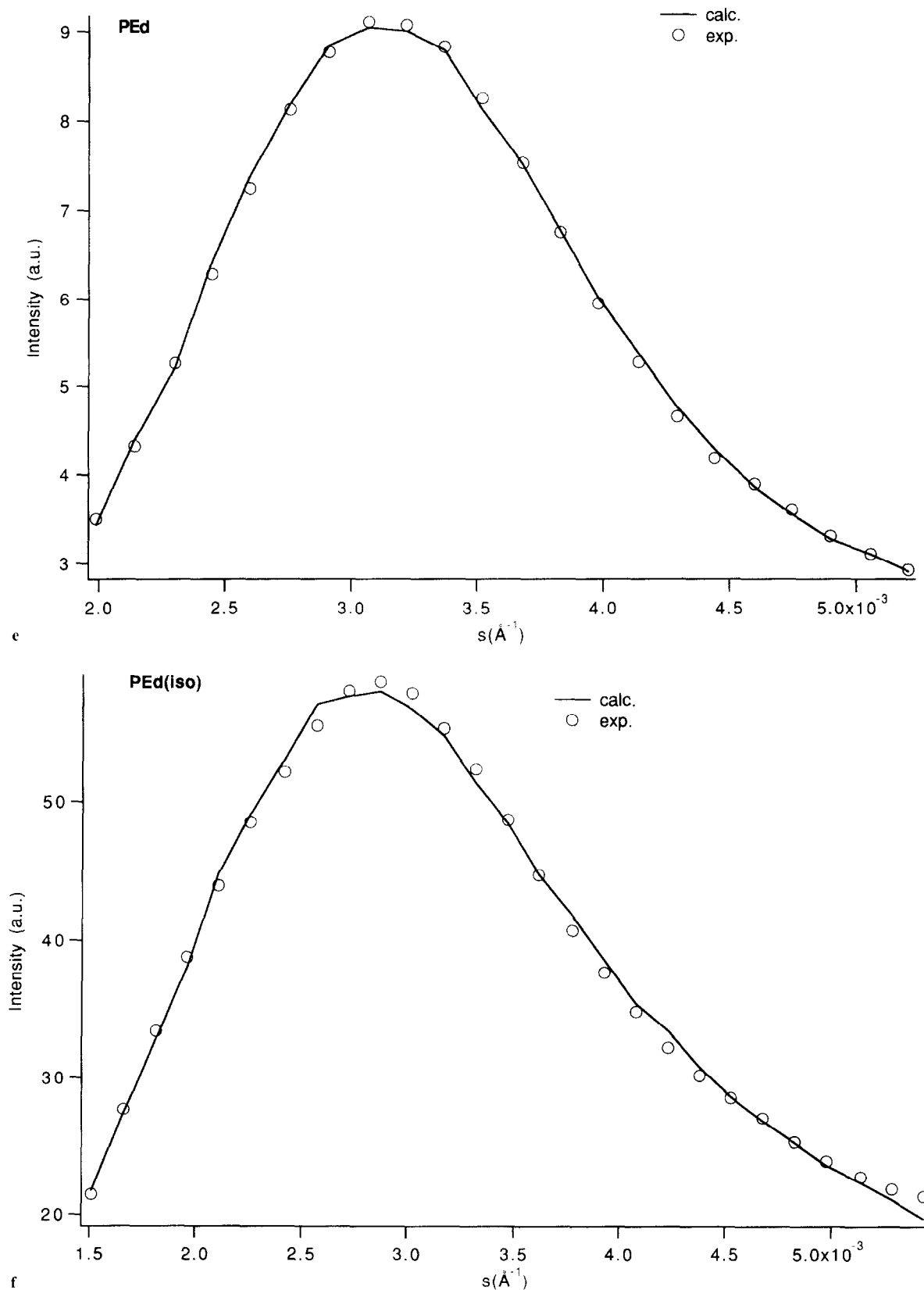


Figure 4 (Continued)

Table 4 Fit parameters obtained for the HDPE samples examined in this study assuming the same (exponential) function for the lamellar distribution

Sample	PEa	PEb	PEc	PEc(iso)	PEd	PEd(iso)
<i>N</i>	14	21	29	∞	43	59
<i>Y</i>	245	250	218	311	246	286
<i>Z</i>	83	81	74	85	90	96
<i>X</i>	328	331	292	396	336	382
Φ	0.746	0.754	0.745	0.786	0.733	0.749
σ_Y	35	35	30	52	44	69
σ_Z	12	11	10	14	16	23
σ_X	37	37	32	54	47	72
σ_Φ	0.06	0.06	0.05	0.07	0.07	0.09
R_{WP}	0.0161	0.0377	0.0297	0.0428	0.0113	0.0170

PEd(iso), and reaches ∞ for PEc(iso). This could indicate the presence of more extended lamellar stacks when the samples are crystallized under isothermal conditions.

CONCLUSIONS

The model which gives the best values for the fitting of the SAXS patterns is the variable stack form, which has $N < 50$ for PE(a-d) (crystallized during cooling), and $N > 50$ for PE(c(iso),d(iso)) (crystallized under isothermal conditions).

The lamellar distributions in the examined HDPE samples seem to be in strict correlation with the molecular-weight distributions and in effect, within the same distribution function, the behaviour of \bar{M}_w/\bar{M}_n and σ_Y and σ_Z is quite similar.

Moreover, it can also be concluded that the fit between the observed and calculated SAXS patterns provides values for both the long-period and crystallinity which show good agreement with those calculated by other methods.

ACKNOWLEDGEMENTS

The authors thank the MURST (Ministero per l'Università e la Ricerca Scientifica e Tecnologica) of

Italy for financial support and the CUGAS (Centro Universitario Grandi Apparecchiature Scientifiche) of the University of Padova for making available the SAXS instrumentation.

REFERENCES

- 1 Blundell, D. J. *Polymer* 1978, **19**, 1258
- 2 Lee, Y. D., Phillips, P. J. and Lin, J. S. *J. Polym. Sci. Polym. Phys. Edn* 1991, **29**, 1235
- 3 Hosemann, R. and Bagchi, S. N. 'Direct Analysis of Diffraction by Matter', North Holland, Amsterdam, 1962, p. 410
- 4 Crist, B. J. *J. Polym. Sci. Polym. Phys. Edn* 1973, **11**, 635
- 5 Strobl, G. R. and Muller, N. J. *J. Polym. Sci. Polym. Phys. Edn* 1973, **11**, 1219
- 6 Vonk, C. G. *J. Appl. Crystallogr.* 1973, **6**, 148
- 7 Wunderlich, B. 'Macromolecular Physics: Crystal Structure, Morphology and Defects', Vol. 1, Academic, New York, 1973, p. 385
- 8 Vonk, C. G. and Pijpers, A. P. *J. Polym. Sci. Polym. Phys. Edn* 1985, **23**, 2517
- 9 Vonk, C. G. *J. Appl. Crystallogr.* 1971, **4**, 340
- 10 Vonk, C. G. *Makromol. Chem. Macromol. Symp.* 1988, **15**, 215
- 11 James, F. and Roos, M. *Comput. Phys. Commun.* 1975, **10**, 343
- 12 Young, R. A. and Prince, E. *J. Appl. Crystallogr.* 1982, **15**, 357